STEM CELLS TRANSLATIONAL MEDICINE®

TISSUE-SPECIFIC PROGENITOR AND STEM CELLS

Dynamic Changes in Brain Mesenchymal Perivascular Cells Associate with Multiple Sclerosis Disease Duration, Active Inflammation, and Demyelination

ELLEN IACOBAEUS [a,b*] RACHAEL V. SUGARS,[c*] ANTON TÖRNQVIST ANDRÉN,[a] JESSICA J. ALM,[a,d] HONG QIAN,[e] JANEK FRANTZEN,[f] JIA NEWCOMBE,[g] KANAR ALKASS,[h] HENRIK DRUID,[h] MATTEO BOTTAI,[i] MATIAS RÖYTTÄ,[d] KATARINA LE BLANC[a,j]

[a]Division of Clinical Immunology, Department of Laboratory Medicine, [b]Department of Clinical Neuroscience, [c]Division of Oral Facial Diagnostics and Surgery, Department of Dental Medicine [d]Department of Pathology, University of Turku and Turku University Hospital, Finland; [e]Center for Hematology and Regenerative Medicine, Department of Medicine, [h]KI Donatum, Department of Forensic Medicine, [i]Unit of Biostatistics, Institute of Environmental Medicine, Karolinska Institutet, Stockholm, Sweden; [f]Division of Clinical Neuroscience, Department of Neurosurgery, University of Turku and Turku University Hospital, Finland; [g]NeuroResource, UCL Institute of Neurology, University College London, London, England, United Kingdom; [j]Hematology Centre, Karolinska University Hospital, Stockholm, Sweden

*Contributed equally.

Correspondence: Ellen Iacobaeus, M.D., Ph.D., Division of Clinical Immunology, Department of Laboratory Medicine and Department of Clinical Neuroscience, Karolinska Institutet, Stockholm, Sweden. Telephone: +46851775314; Fax: +46851773757; e-mail: ellen.iacobaeus@karolinska.se

Received February 2, 2017; accepted for publication July 5, 2017; first published September 23, 2017.

http://dx.doi.org/10.1002/sctm.17-0028

Key Words. Multiple sclerosis • Neuroinflammation • Central nervous system • Mesenchymal stromal cell • Pericyte • Perivascular niche • Blood vessels

ABSTRACT

Vascular changes, including blood brain barrier destabilization, are common pathological features in multiple sclerosis (MS) lesions. Blood vessels within adult organs are reported to harbor mesenchymal stromal cells (MSCs) with phenotypical and functional characteristics similar to pericytes. We performed an immunohistochemical study of MSCs/pericytes in brain tissue from MS and healthy persons. Post-mortem brain tissue from patients with early progressive MS (EPMS), late stage progressive MS (LPMS), and healthy persons were analyzed for the MSC and pericyte markers CD146, platelet-derived growth factor receptor beta (PDGFRβ), CD73, CD271, alpha-smooth muscle actin, and Ki67. The MS samples included active, chronic active, chronic inactive lesions, and normal-appearing white matter. MSC and pericyte marker localization were detected in association with blood vessels, including subendothelial $CD146^+PDGFR\beta^+Ki67^+$ cells and $CD73^+CD271^+PDGFR\beta^+Ki67^-$ cells within the adventitia and perivascular areas. Both immunostained cell subpopulations were termed mesenchymal perivascular cells (MPCs). Quantitative analyses of immunostainings showed active lesions containing increased regions of $CD146^+PDGFR\beta^+Ki67^+$ and $CD73^+CD271^+PDGFR\beta^+Ki67^-$ MPC subpopulations compared to inactive lesions. Chronic lesions presented with decreased levels of $CD146^+PDGFR\beta^+Ki67^+$ MPC cells compared to control tissue. Furthermore, LPMS lesions displayed increased numbers of blood vessels harboring greatly enlarged $CD73^+CD271^+$ adventitial and perivascular areas compared to control and EPMS tissue. In conclusion, we demonstrate the presence of MPC subgroups in control human brain vasculature, and their phenotypic changes in MS brain, which correlated with inflammation, demyelination and MS disease duration. Our findings demonstrate that brain-derived MPCs respond to pathologic mechanisms involved in MS disease progression and suggest that vessel-targeted therapeutics may benefit patients with progressive MS. STEM CELLS TRANSLATIONAL MEDICINE *2017;6:1840–1851*

SIGNIFICANCE STATEMENT

This immunohistochemical study characterized vascular cells phenotypically similar to pericytes and mesenchymal stromal cells (MSCs) in brain tissue of multiple sclerosis (MS) and healthy persons. We found variations in phenotype, distribution, and proliferation of cells co-expressing markers for MSCs and pericytes that associated with inflammation and MS disease duration. Tissue from long standing MS presented with increased numbers of blood vessels that harbored expanded perivascular areas of cells staining positive for MSCs/pericyte markers. This is the first study to show involvement of MSC/pericyte phenotypic changes in MS pathology and highlights that vessel-targeted treatments may benefit late stage MS.

INTRODUCTION

Multiple sclerosis (MS) is a chronic inflammatory demyelinating disease of the central nervous system (CNS). Pathologically, MS presents with the formation of multiple focal lesions in the CNS that often develop around blood vessels associated with breakdown of the blood-brain barrier (BBB), inflammatory cells, demyelination, axonal damage, and glial scarring [1]. The BBB, including specialized endothelial cell tight junctions in conjunction with pericytes, provides a highly protective barrier under healthy conditions [2, 3]. A significant dysregulation of the BBB associated with lymphocyte recruitment into the CNS represents a crucial event in MS disease pathogenesis

[4]. Prominent vascular changes in MS were observed in early neuropathological reports [5], and recently angiogenesis and increased blood vessel density have been reported in MS cerebral white matter [6]. Neuronal tissues, such as the brain, are recognized to possess the highest density of pericytes surrounding blood vessels in the body [5, 6]. Pericyte depletion studies have revealed key functions in the regulation of BBB integrity and previous studies demonstrate an important role for pericytes in immunological responses and repair mechanisms in the CNS [3, 7–9]. In addition, pericytes have been reported to possess multipotent potential, differentiating down the mesenchymal lineages in vitro [10–12]. Recent reports have suggested that mesenchymal stromal cells (MSCs) may represent a subclass of pericytes following their identification in the perivascular tissue of almost all organs of the human body, including the adult brain [13–15]. In vitro, MSCs, in addition to their multipotency are characterized by their capacity to exert strong immunosuppressive and trophic properties, mainly by the secretion of soluble factors [16]. Consequently, in vitro expanded MSCs have been used experimentally as an anti-inflammatory cell-based therapy for various diseases, including MS [17, 18]. A large number of in vitro studies have described the immunoregulatory and regenerative effects mediated by MSCs. Indeed evidence from the animal model of MS, experimental autoimmune encephalomyelitis (EAE), suggests that intravenous administration of MSCs reduces demyelination, mediates neuroprotection, and diminishes CNS leukocyte infiltration [19, 20]. However, knowledge is limited regarding the biological relevance of in vivo MSCs in the human CNS, and detailed studies exploring MSCs in post-mortem brain tissue has not been performed. In vitro, a molecular signature consisting of positive expression for CD70, CD90, and CD105 but absence of CD34, CD45, CD14, CD116, CD796, CD19, and HLA-DR defines culture-expanded MSCs [21]. At present, no specific marker or marker panel has been established to determine true in vivo MSCs within human tissues. In addition, pericytes lack a single specific marker and are usually identified by a combination of surface markers, such as melanoma cell adhesion molecule (CD146), platelet-derived growth factor receptor beta (PDGFRβ, alpha-smooth muscle actin (α-SMA), and chondroitin sulfate proteoglycan 4 (NG2), and their anatomical location [3, 13, 22, 23]. However, marker expression is dynamic and depends on the developmental stage, tissue origin, and in vivo/in vitro milieu [24]. Since MSCs have similarities with pericytes, it has been argued that the pericyte may be the true in vivo equivalent to the in vitro MSC phenotype [13].

In view of the importance of pericytes in maintaining the integrity of the BBB, and the immunoregulatory and regenerative properties of MSCs and pericytes, we hypothesized that the phenotype, activity, and distribution of vascular cells resembling MSCs and/or pericytes, herein referred to as mesenchymal perivascular cells (MPCs), may be altered with disease activity in MS. To this end, we analyzed MS brain tissue from early stage progressive MS (EPMS; disease duration $<$10 years) in comparison with late stage progressive MS (LPMS; disease duration $>$17 years) and healthy control brain tissue. Using an array of MSC and pericyte markers we identified two MPC populations associated with vessels in both MS and healthy control brain tissue. Immunoreactivity of MSC and pericyte markers, in addition to proliferative activity were significantly altered between EPMS and LPMS, and varied between MS lesions with different inflammatory and demyelinating activity. Our findings suggest that brain MPCs associated with blood vessel walls respond to disease processes in MS lesions. Increased understanding of the localization of MPCs in the brain of MS and healthy tissues will advance our knowledge about disease specific molecular and cellular changes and may provide new insights into the development of vessel-targeted therapies for MS patients.

Materials and Methods

Ethical Considerations and Permissions

Procedures involving human participants were in accordance with the ethical standards of the Regional Ethics Review Board, Stockholm, (Dnr: 2014/822–31/4), and the University of Turku, Finland (ETML: 14/1803/2016), within the 1964 Helsinki Declaration and its amendments. For this type of study formal consent was not required. Samples were also provided by the NeuroResource tissue bank, University College London (UCL) Institute of Neurology, London, England. (NR LB 06–2015), with informed consent documentation approved by NHS London Research Ethics Committees, and tissue samples stored under a Licence from the U.K. Human Tissue Authority (HTA).

Patient Material

Post-mortem formalin-fixed paraffin embedded (FFPE) brain blocks from EPMS patients (6 secondary progressive MS, SPMS), aged 40 years (range 29–52 years) with disease duration $<$10 years (mean 7.5 years, range 7–10 years) were provided by the NeuroResource tissue bank, UCL Institute of Neurology. FFPE LPMS patients (8 SPMS and 4 primary progressive, PPMS), aged 60 years (range 40–85 years) with disease duration $>$17 years (mean 33 years, range 17–40 years) were provided by the Department of Neuropathology, University of Turku. MS cases were selected retrospectively based on clinical and neuropathological diagnoses. Overall 48 MS tissue blocks from periventricular areas, subcortical white matter regions of the frontal lobe, parietal lobe and occipital lobe were examined. Post-mortem healthy control brain tissue, collected by Karolinska Institutet Donatum, included 16 blocks from 8 patients (mean age 43 years, range 22–59 years), from subcortical white matter of frontal and occipital lobes. Detailed patient and tissue information are provided in Table 1; Supporting Information Table 1. All brains have been neuropathologically screened to exclude confounding pathologies. Dissected brain tissues were fixed in 4% (wt/vol) formalin, dehydrated, and embedded in paraffin. Four micrometer thin sections of MS or healthy tissue were mounted on Superfrost Plus slides (Menzel-Gläser, Braunschweig, Germany, http://www.thermofisher.com/de/de/home.html). Sections were deparaffinized in xylene and rehydrated through a graded series of alcohols prior to subsequent analysis.

Routine Pathological Analyses and Classification of MS Tissue

Sections were routinely stained with Mayer's hematoxylin and eosin and Luxol fast blue using the Ventana HE 600 System (Ventana Medical Systems, Roche Group, Tucson, http://www.ventana.com). An antibody targeted against CD68 (Supporting Information Table 2) was stained using the BenchMark XT (Roche Group) automatic stainer system at the Department of Pathology, University of Turku. CD4, CD8, and myelin basic protein (MBP; Supporting Information Table 2) stainings were performed as outlined below. Sections were digitalized on a 3D Histech Midi Scanner System (Histolab Products AB, Gothenburg, Sweden). Histological findings

Table 1. Demographics of MS patients and healthy persons included within the study

Sample code	Gender	Age (years)	MS Subdiagnosis	MS disease duration (years)	Death-autopsy interval	Cause of death
EPMS1	F	42	SPMS	10	34 hours	Pneumonia
EPMS2	F	37	SPMS	10	24 hours	Pneumonia
EPMS3	F	47	SPMS	7	16 hours	Myocardial infarction
EPMS4	F	29	SPMS	8	11 hours	Pneumonia
EPMS5	M	52	SPMS	7	29 hours	Pneumonia
EPMS6	F	29	SPMS	7	14 hours	Pneumonia
LPMS1	F	85	SPMS	40	4 day	Urosepsis
LPMS2	M	64	PPMS	30	6 days	Pneumonia
LPMS3	M	60	PPMS	34	3 days	Respiratory failure
LPMS4	F	51	SPMS	33	5 days	Pneumonia
LPMS5	F	69	SPMS	39	6 days	Choking
LPMS6	F	45	SPMS	24	1 day	Breast cancer
LPMS7	M	60	SPMS	36	5 days	Pneumonia and sepsis
LPMS8	M	40	PPMS	20	2 days	Pneumonia
LPMS9	F	52	SPMS	35	3 days	Pneumonia and sepsis
LPMS10	M	81	SPMS	33	2 days	Pneumonia
LPMS11	F	51	PPMS	17	4 days	Pnemonia
LPMS12	F	73	SPMS	27	1 day	Breast cancer
HC1	M	22	n.a	n.a	24 hours	Undetermined
HC2	M	25	n.a	n.a	48 hours	Hanging
HC3	M	47	n.a	n.a	60 hours	Hanging
HC4	M	36	n.a	n.a	48 hours	Drug intoxication
HC5	F	59	n.a	n.a	24 hours	GI bleeding
HC6	M	45	n.a	n.a	25 hours	Pulmonary embolism
HC7	M	54	n.a	n.a	63 hours	Hanging
HC8	M	55	n.a	n.a	58 hours	Drug intoxication

Abbreviations: EPMS, early progressive; F, female; GI, gastrointestinal; HC, healthy control; LPMS, late-stage progressive MS; M, male; n.a, not applicable; PPMS, primary progressive MS; SPMS, secondary progressive MS.

in each section were examined by three experts and lesions classified as active, chronic active and chronic inactive as described below. Macroscopically normal-appearing white matter (NAWM) was defined by localization at least 1 cm from the visible lesion edge.

Immunohistochemical Staining

The immunohistochemical protocol was adapted from Sugars et al. [25]. Rehydrated sections were pretreated according to the parameters described in Supporting Information Table 2 for the respective antibodies. Sections were rinsed in Tris buffered saline (50 mM Tris, 150 mM sodium chloride, pH 7.6, with 0.01% (vol/vol) Tween 20 (TBST; Sigma Aldrich, Stockholm, Sweden, http://www.sigmaaldrich.com). All sections were treated with 3% (vol/vol) hydrogen peroxide for 5 minutes at room temperature. Nonspecific binding was blocked using 10% (vol/vol) normal rabbit or goat serum (DAKO, Glostrup, Denmark, http://www.agilent.com), 0.3% (vol/vol) Triton-X-100 (Sigma), and 0.1% (wt/vol) cold water fish gelatin (Sigma) for 1 hour at room temperature, followed by incubation with the corresponding primary antibody (Supporting Information Table 2) prepared in 4% (vol/vol) normal serum at 4°C overnight. Control experiments were performed with either the corresponding IgG isotype (Vector Laboratories Ltd., Peterborough, U.K., https://vectorlabs.com/uk/7) or with omission of the primary antibody (Supporting Information Table 2). The sections were rinsed three times in TBST for 5 minutes and subsequently probed with 1:500 biotinylated secondary antibody (Vector Laboratories Ltd.), prepared in 4% (vol/vol) normal serum, for 1 hour at room temperature. Following washing, enhancement with the ABC Elite Horseradish Peroxidase (HRP) kit (Vector Laboratories Ltd.) was performed according to the manufacturer's instructions. Bound antibody was detected using the 3,3′-diaminobenzidine (DAB) substrate (DAKO) for HRP and the signal developed for an optimized time period. Sections were counterstained for 10 seconds with Mayer's Hematoxylin, followed by dehydration and mounting in Pertex (Histolab Products AB).

Digital Image Analysis of Immunohistochemical Staining with Complementary Statistical Analyses

All stained slides were scanned and digitalized using the 3D Histech Scanner and viewed within the Panoramic Viewer Software 1.15 (3D Histech). Serial sections from the respective antibodies were aligned using Case Viewer (3D Histech) and multiple fields of view (FoV) were taken from annotated regions by one team member. To standardize the FoV, every image contained at least

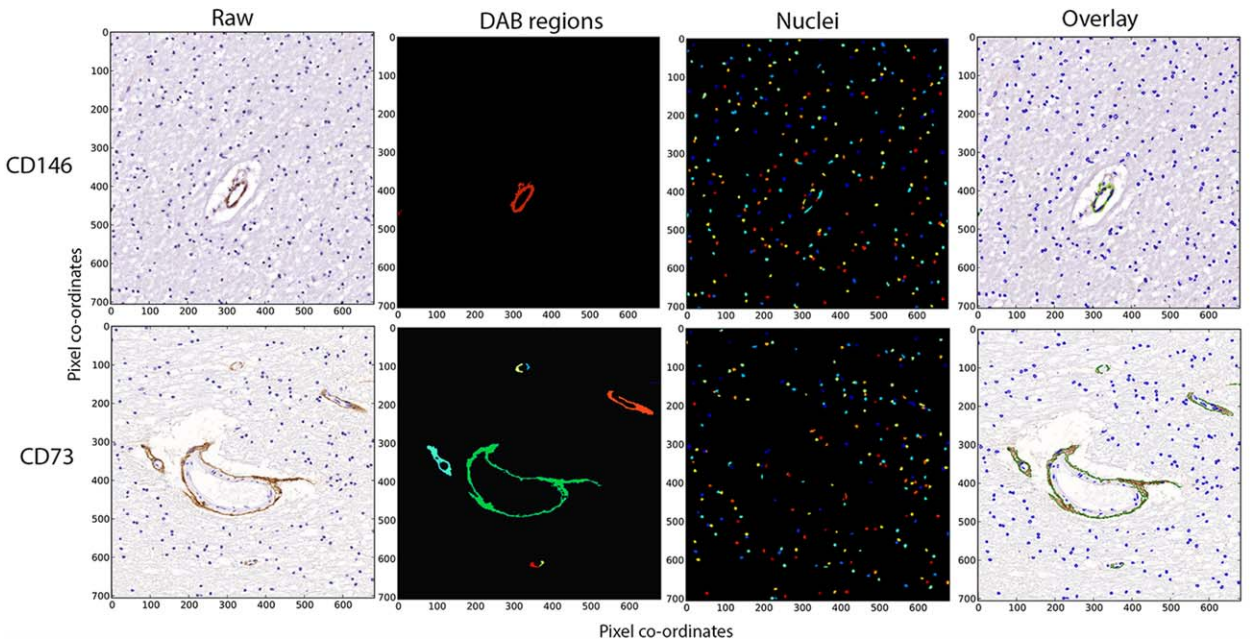

Figure 1. Image analysis workflow. Quantification of mesenchymal stromal cell/pericyte markers was performed using the CellProfiler image analysis software, and workflows were established for each respective antibody (representative CD146 and CD73 are shown). Fields of view were taken from the original image (Raw) and using the program threshold algorithms DAB stained regions (DAB regions) and nuclei (Nuclei) were defined (colored objects were arbitrarily assigned). Pixel area was determined from the colored segments detected in the DAB regions and nuclei. The images represent individual areas detected with either DAB or nuclei staining. These identified regions were subsequently overlaid on the original field of view to allow for validation (Overlay). *x*- and *y*-axes represent pixel co-ordinates of the original images. Abbreviation: DAB, 3,3′-diaminobenzidine

one vessel. Annotated regions were defined within a lesion, in macroscopically NAWM and healthy tissues. A minimum of 10 FoV were taken from each region at ×20 magnification on a 1,366 × 768 sized screen = 683 × 706 dots per inch, (dpi)/image. Quantification of immunolocalization of the markers CD73, CD271, PDGFRβ, CD146, and Ki67 was performed using the open-source CellProfiler Software version 2 (http://www.cellprofiler.org) (representative images of the process are detailed in Fig. 1) [26]. Within the program, workflows were established for each respective antibody. Original FoV were converted to gray scale to allow segmentation and identification of stained objects (colored objects were arbitrarily assigned) using the programs threshold algorithms. Filters were applied to include DAB stained region objects and nuclei, and to exclude anything that may represent debris. Output images were manually inspected to facilitate optimization of the program settings. Multiple measurements were made on the segmented identified objects, including total stained pixel area and total pixel area per image.

Total stained pixel area/total pixel area was analyzed for each image across combinations of stage (EPMS and LPMS) and type of lesion (active, chronic active, chronic inactive, and NAWM) for each of the markers (CD146, PDGFRβ, Ki67, CD73, and CD271) separately. We used generalized estimating equations with an independent working correlation matrix to take the potential intrasubject correlation into account when estimating the standard errors [27]. We adopted a gamma distribution family with a log-link, as the total pixel area showed a positive and skewed distribution in each of the considered groups. The results are reported as pixel-area fold-change with 95% confidence intervals, p values $<.05$ were considered statistically significant. All analyses were performed with Stata version 14 (StataCorp, College Station, TX, https://www.stata.com/company/).

Quantification of Vessels

Vessel number was quantified for EPMS and LPMS, including regions of active, chronic active, chronic inactive and NAWM tissue, in addition to healthy control brain white matter (five cases). Serial sections stained with CD31 and α-SMA were digitally scanned using the 3D Histech Slide Scanner as described above. FoV representing lesions, NAWM or healthy tissue were identified and the number of vessels positive for CD31 and α-SMA manually counted within the specified area. The number of capillaries was determined from the $CD31^+$ and $\alpha\text{-SMA}^-$ population based on previous findings reporting negative immunoreactivity of α-SMA in adult human brain capillaries [24, 28]. All quantification studies were performed by three separate individuals on three separate occasions under standardized conditions. Statistical significance for the total number of vessels across the stage (EPMS, LPMS, and healthy) and lesion type (active, chronic active, chronic inactive, and NAWM) was assessed as above using generalized estimating equations with an independent working correlation matrix that again took into consideration potential intra-subject correlation during the estimation of standard errors. Calculations were performed with Stata version 14 (Stata Corp) with p values $<.05$ considered as significant.

Results

MS Lesion Characterization

Characterization of demyelinating and inflammatory activity of MS lesions was assessed using hematoxylin and eosin and Luxol Fast Blue staining, immunolocalization of macrophages/microglia (CD68) and infiltrating lymphocytes (CD4 and CD8), and MBP

(Supporting Information Fig. 1). A total of 14 active lesions, 25 chronic active lesions, 7 chronic inactive lesions, and 12 NAWM were included in the study. Data on tissue distribution between EPMS and LPMS is provided in Supporting Information Table 1. Classification of lesions was performed according to published criteria [29]. Active lesions were characterized by indistinct borders on Luxol Fast Blue staining and abundant lipid-laden $CD68^+$ macrophages/microglia (occasionally MBP positive) throughout the total lesion areas. Chronic active lesions displayed restriction of $CD68^+$ cells to the lesion border. Inactive lesions contained a hypocellular demyelinated tissue and a sharp demarcated border from the NAWM. Examination of CD4 and CD8 staining across all tissues detected lymphocytes in the MS sections in the perivascular area and occasionally within the parenchyma associated with active and chronic active lesions.

Detection of Two Separate Populations of MPCs in MS and Healthy Control Brain Tissue

Immunohistochemical analysis of the MSC markers CD73 (ecto-5′-nucleotidase) and CD271 (p75-neurotrophin receptor), and pericyte markers, PDGFRβ and CD146 (also considered an MSC marker), was performed on all brain tissue blocks. Serial section staining identified co-expression of more than one MPC marker exclusively in the vasculature and perivascular area of the brain tissue (Fig. 2; Supporting Information Figs. 2, 3). Two separate MPC populations associated with cerebral vessels were identified based on marker expression and vessel wall distribution, in MS and healthy control tissue. The innermost MPC population with a sub-endothelial vascular localization, separated from the $CD31^+$ endothelial cell layer, displayed positive immunostaining for CD146 and PDGFRβ but not for CD73 and CD271 (Fig. 2; Supporting Information Figs. 2, 3). Second, another population defined as $CD73^+CD271^+PDGFR\beta^+$ was detected in the adventitia layer and perivascular tissue (Fig. 2; Supporting Information Figs. 2, 3). Proliferative activity, evidenced by detection of positive Ki67 immunostaining, was found within $CD146^+PDGFR\beta^+$ regions but not in adventitial/perivascular $CD73^+CD271^+PDGFR\beta^+$ domains in the corresponding vessels (Fig. 3A; Supporting Information Figs. 2, 3). In the smallest vessels and capillaries, distinct differences in distribution of the two MPC populations were impossible to visualize and a codistribution was observed.

Increased Localization of $CD146^+PDGFR\beta^+$ and $CD73^+CD271^+PDGFR\beta^+$ was Associated with Inflammatory and Demyelinating Activity

Digital image analysis of the immunohistochemistry staining's, based on measurements of total area occupied by stain, revealed significant differences between healthy control and MS brain tissue, in addition to significant variations between lesions with diverse pathological classification (Fig. 2; Supporting Information Fig. 2, Table 3). A major pattern in MS was the increased localization of cells positive for MSC/pericyte markers associated with ongoing inflammation and demyelination (active and chronic active lesions) compared to inactive lesions. EPMS active lesions had increased localization of PDGFRβ (5-fold, $p < .001$) and CD73 (2-fold, $p = .020$) compared to chronic inactive lesions. No significant changes in Ki67 were apparent for EPMS between different lesion types (Fig. 3B; Supporting Information Table 3). In LPMS, active lesions displayed enhanced positivity for CD146 (8-fold, $p < .001$), PDGFRβ (3-fold, $p < .001$), CD73 (4-fold, $p < .001$), and CD271 (8-fold, $p < .001$) compared to inactive lesions (Supporting Information Table 3). This was reflected in the comparison of chronic active lesions compared to inactive lesions in LPMS (CD146, 5-fold, $p < .001$; CD73, 2-fold, $p = .015$, and CD271, 5-fold, $p < .001$, Figs. 4A, 4C, 4D; Supporting Information Table 3). Ki67 was also significantly increased in active (3-fold, $p = .008$) and chronic active lesions (3-fold, $p = .001$) compared to inactive lesions in LPMS (Fig. 3B; Supporting Information Table 3). In order to investigate immunogenicity of the two distinct MPC populations and a possible correlation with inflammatory activity, we performed immunohistochemical staining for HLA-DR on MS lesions, NAWM, and healthy control tissue. HLA-DR positive staining was detected in the adventitia and perivascular $CD73^+CD271^+$ regions, and not in the subendothelial MPC layer, in active MS lesions of both EPMS and LPMS and in some immune cells within the vessel areas (Supporting Information Fig. 4). MPCs of chronic active, chronic inactive lesions, and NAWM were negative for HLA-DR immunoreactivity in both EPMS and LPMS. Little or no detection of HLA-DR was found in MPCs of the healthy brain tissue (Supporting Information Fig. 4).

Loss of $CD146^+PDGFR\beta^+$ MPCs in Chronic Active and Inactive MS Lesions Compared to Healthy Control Tissue

Chronic active and chronic inactive lesions obtained from MS subgroups (EPMS and LPMS) demonstrated a pronounced decrease in localization of CD146 and PDGFRβ (Figs. 4A, 4B), compared to healthy control tissue. In EPMS, CD146 decreased 3-fold in active lesions ($p < .01$), 11-fold in chronic active ($p < .001$), and 5-fold in chronic inactive ($p < .001$) lesions, while in LPMS chronic inactive lesions displayed a 6-fold decrease ($p < .001$) compared to healthy tissue (Fig. 4A; Supporting Information Table 3). PDGFRβ decreased 4-fold in both chronic active and chronic inactive lesions from EPMS ($p < .001$ for both), and 2-fold in chronic active ($p < .001$) and chronic inactive ($p = .009$) lesions from LPMS (Fig. 4B), compared to healthy control tissue.

Enlarged $CD73^+CD271^+$ Adventitial and Perivascular Domains Across All MS Lesions in LPMS Compared to Healthy Control Tissue

Vessels within EPMS tissue lesions presented with enlarged $CD73^+$ regions in active (4-fold, $p < .001$), chronic active (2-fold, $p < .05$), and inactive lesions (2-fold, $p < .01$) compared to healthy tissue (Fig. 4C; Supporting Information Table 3). This finding was even more pronounced in LPMS where a highly significant increase in perivascular $CD73^+CD271^+$ cells were detected in all lesions; CD73 was enriched 14-fold ($p < .001$) in active, 6-fold ($p < .001$) in chronic active lesions and 4-fold ($p < .001$) in chronic inactive compared to healthy controls, and CD271 increased 20-fold ($p < .001$) in active lesions, 11-fold ($p < .001$) in chronic active lesions and 2-fold ($p < .001$) in chronic inactive lesions compared to healthy tissue (Figs. 4C, 4D; Supporting Information Table 3).

Increased Detection of $CD146^+PDGFR\beta^+$ and $CD73^+CD271^+PDGFR\beta^+$ MPCs in Cerebral Vessels of LPMS Compared to EPMS

Comparative analyses between different disease durations (EPMS and LPMS) were used to assess potential differences in MPC marker dynamics and proliferative activity in lesions with similar neuropathological classification (Figs. 2 and 4; and Supporting Information Table 3). LPMS active lesions, evaluated against EPMS active lesions, contained vascular tissue with increased CD146 (4-fold, $p = .004$) and CD73 (3-fold, $p < .001$) distribution, while

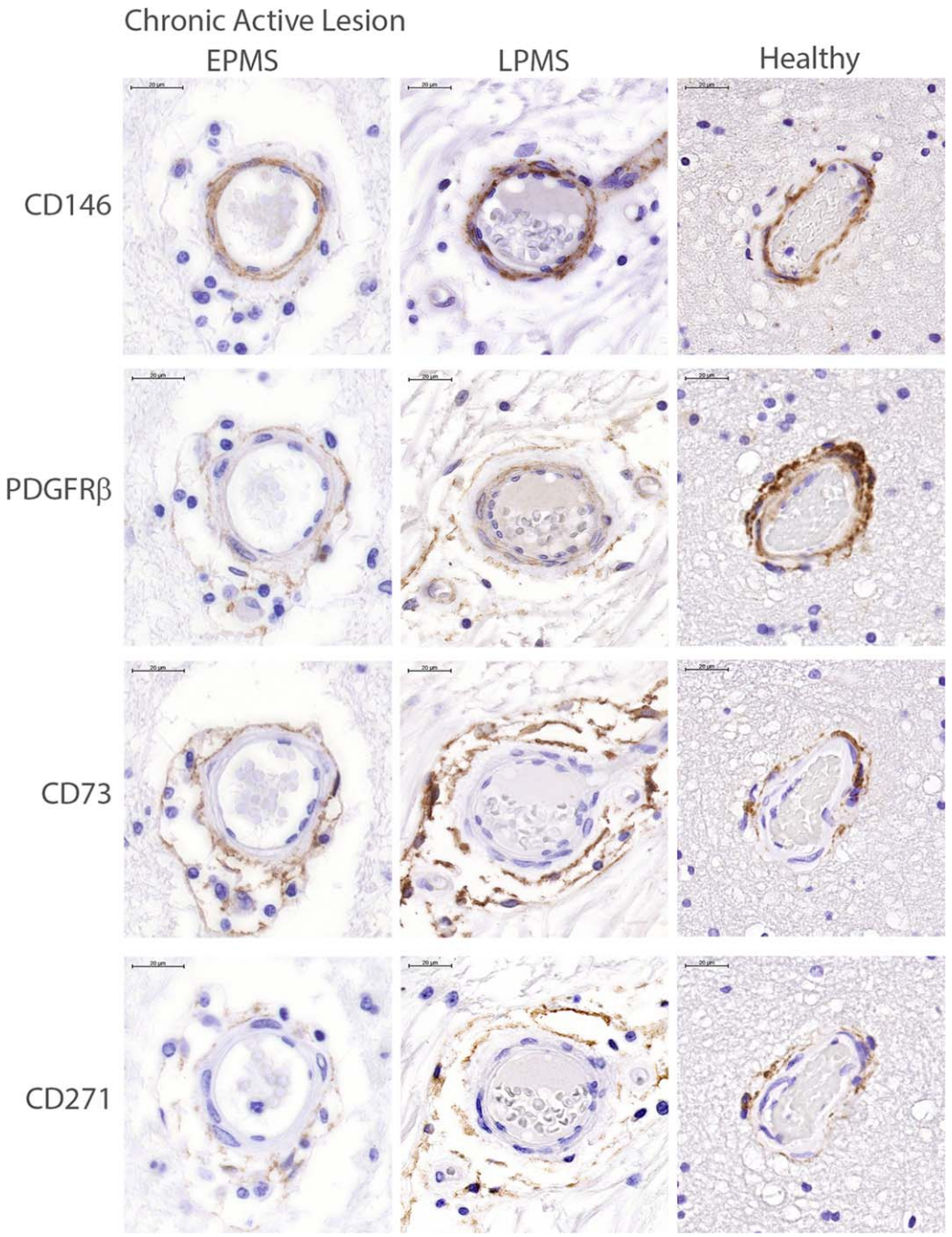

Figure 2. Localization of mesenchymal stromal cell (MSC)/pericyte markers in MS and healthy control brain tissue. Immunohistochemical staining of serial sections for MSC/pericyte markers localized to the perivascular regions in the adult healthy control brain in chronic active lesions from EPMS and LPMS, as well as healthy tissues (representative images of disease status across all donors). CD73, CD271, and PDGFRβ were found typically within the adventitial layer and perivascular tissue, whereas pericyte markers CD146 and PDGFRβ were localized abluminally to endothelial cells. Scale bars = 20 μm. Abbreviations: EPMS, early progressive MS; LPMS, late stage progressive MS; PDGFRβ, platelet-derived growth factor receptor beta.

no changes in PDGFRβ localization were apparent. Compared to EPMS chronic active lesions, LPMS chronic active lesions presented with a significant enhancement of all MSC/pericyte markers (CD146, 9-fold, $p < .001$; PDGFRβ, 2-fold, $p < .001$; CD73, 4-fold, $p < .001$ and CD271, 8-fold, $p < .001$). Furthermore, in chronic inactive LPMS lesions an increased localization of PDGFRβ (3-fold, $p = .001$) and CD73 (2-fold, $p = .032$), but no change in CD146 and CD271 were detected compared to EPMS (Fig. 4). Increased proliferation (Ki67) was recorded in both active (5-fold, $p = .001$) and chronic active (3-fold, $p < .001$) lesions of LPMS compared to EPMS (Fig. 3B; Supporting Information Table 3).

Changes in MPC Marker Localization and Proliferative Activity in NAWM Tissue

Vessels within NAWM exhibited a similar pattern of MPC distribution to that described above including the innermost

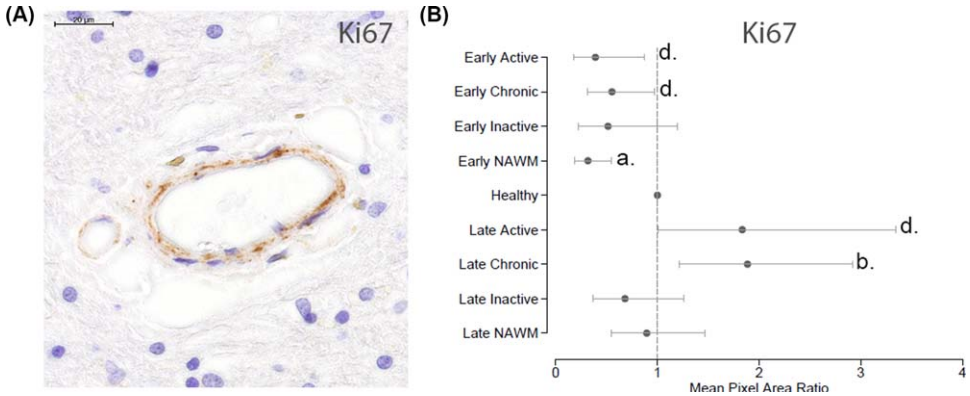

Figure 3. Analysis of cell proliferation using Ki67. **(A):** Ki67 localization resembled a similar pattern detected for the markers CD146 and platelet-derived growth factor receptor beta. Scale bar = 20 μm. **(B):** In early progressive MS (EPMS) quantification of Ki67 staining demonstrated decreased proliferative activity in active lesions and in NAWM compared to healthy tissue (dotted line normalized to 1). Late stage progressive MS (LPMS) displayed increased proliferative activity in chronic active lesions compared to healthy control tissue. When comparing LPMS with EPMS it was observed that the proliferative activity was amplified in active, chronic active and NAWM lesions of LPMS compared to EPMS. *p* values a = ≤.001, b = ≤.01, and c = ≤.05. Abbreviation: NAWM, normal-appearing white matter.

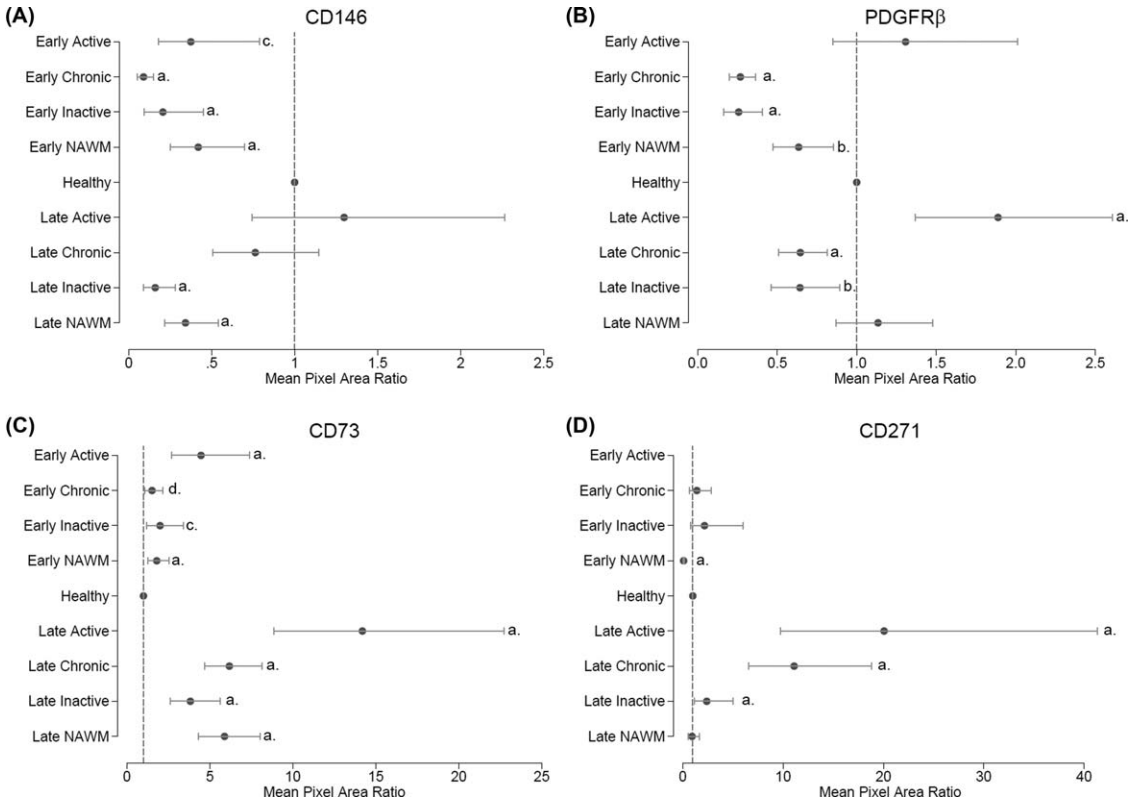

Figure 4. Quantification of mesenchymal perivascular cells localization by image analysis in early progressive MS (EPMS) and late stage progressive MS (LPMS). Quantification of immunohistochemical staining for mesenchymal stromal cells/pericyte markers using generalized estimating equations demonstrated significant changes in mean pixel area ratio (fold-change) stained between different MS tissue types and healthy, and demyelinating disease and healthy. A significant difference in marker detection between EPMS and LPMS tissues was also apparent. **(A):** CD146, **(B):** PDGFRβ, **(C):** CD73, and **(D):** CD271. Detailed numbers pertaining to the significance can be found in Supporting Information Table 3. *p* values a = ≤.001, b = ≤.005, c = ≤.01, and d = ≤ .05. The dotted line indicates the normalized value (1) of healthy tissue. Abbreviations: NAWM, normal-appearing white matter; PDGFRβ, platelet-derived growth factor receptor beta.

$CD146^+PDGFR\beta^+Ki67^+$ and the outer $CD73^+CD271^+PDGFR\beta^+$ $Ki67^-$ populations detected in the adventitial layer and perivascular tissue. Quantitative image analyses revealed major differences between MS and healthy tissue, and between EPMS and LPMS MS subgroups (Fig. 4; Supporting Information Figs. 2, 3, and Table 3). NAWM tissue from EPMS was characterized by a pronounced decrease in the immunolocalization of CD146 (2-fold, $p < .001$, PDGFRβ (2-fold, $p = .003$) and CD271 (11-fold, $p < .001$), while

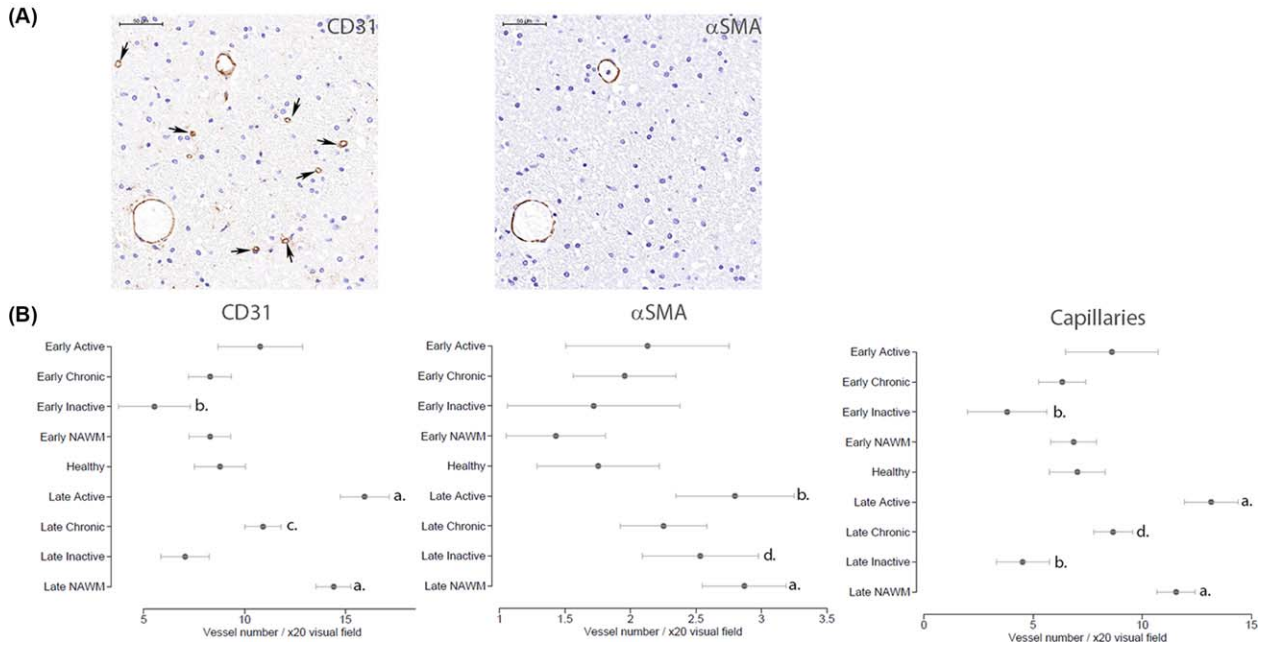

Figure 5. Vessel density changes between stages of multiple sclerosis (MS) and MS tissue type compared to healthy controls. **(A):** Vessels were detected in the MS and healthy brain tissue using CD31 and α-SMA immunolocalization. Arrows point to capillaries, designated as $CD31^{+}\alpha\text{-}SMA^{-}$ vessels. Scale bars = 20 μm. **(B):** Semiquantification of vessels positive for CD31 and α-SMA were manually counted, as described in the Materials and Methods, and capillaries determined from the subtraction of α-SMA from CD31. Statistical analysis by generalized estimating equations demonstrated significant differences with respect to the number of total $CD31^{+}$ vessels and capillaries, between MS tissue type and between EPMS and LPMS with healthy tissue. *p* values a = ≤.001, b = ≤.005, c = ≤.01 and d = ≤.05. The dotted line indicates the normalized value (1) of healthy tissue. Abbreviation: α-SMA, alpha-smooth muscle actin.

CD73 distribution increased (2-fold, $p < .001$) compared to healthy control vessels. Vascular tissues of NAWM obtained from LPMS demonstrated decreased detection of CD146 (3-fold, $p < .001$) but increased localization of CD73 (6-fold, $p < .001$), but no change in either PDGFRβ or CD271 compared to healthy control tissue was detected. Ki67 significantly decreased in NAWM in EPMS tissue compared to healthy tissue (3-fold, $p < .001$), whereas NAWM of LPMS showed comparable Ki67 levels. However, comparison of LPMS NAWM against EPMS demonstrated an increased Ki67 localization (3-fold, $p < .001$; Fig. 3B; Supporting Information Table 3) in LPMS.

Amplified Numbers of Blood Vessels in LPMS Tissue Compared to EPMS and Healthy Control Tissue

Quantification and definition of blood vessel numbers within MS and healthy brain tissue was assessed by manual counting of the total number of $CD31^{+}$ and $\alpha\text{-}SMA^{+}$ vessels respectively (Fig. 5A). In EPMS, NAWM, active, and chronic active lesions, a similar number of $CD31^{+}$ blood vessels were seen when evaluated against healthy brain tissue (Fig. 5B; Supporting Information Table 3). EPMS chronic inactive lesions demonstrated a reduced number of $CD31^{+}$ blood vessels compared to healthy control (mean difference = −3-fold, $p = .003$). By contrast, $CD31^{+}$ vessels in LPMS were significantly increased in active lesions (mean difference = 7-fold, $p < .001$), chronic active lesions (mean difference = 2-fold, $p = .007$), and NAWM (mean difference = 6-fold, $p < .001$). LPMS inactive lesions displayed comparable levels of $CD31^{+}$ vessels to that of healthy tissue. A positive correlation between numbers of capillaries ($CD31^{+}\alpha\text{-}SMA^{-}$) and total vessel numbers was found, supported by the increase in capillaries in LPMS active lesions (mean difference = 6-fold, $p < .001$), chronic active lesions (mean difference = 2-fold, $p = .040$), and NAWM (mean difference = 5-fold, $p < .001$) compared to healthy (Fig. 5B; Supporting Information Table 3). EPMS and LPMS chronic inactive lesions were both found to have a reduced number of capillaries compared to healthy control (EPMS mean difference = −3-fold, $p = .004$; LPMS mean difference = −3-fold, $p = .005$).

Discussion

Current knowledge on regenerative and immunosuppressive properties of MSCs has been mainly based on in vitro cultures, while data on the native identity and in vivo function remain sparse (16), [30]. Within this study, we demonstrate the localization of cells co-expressing classical MSC and/or pericyte markers in the human brain, in association with cerebral blood vessels. In line with our data, previous studies have reported the presence of subpopulations of vascular cells with features of MSCs/pericytes in human organs [31, 32]. Studies on muscle, pancreatic, and adipose tissue have demonstrated two separate vascular MSC progenitors, including tunica media $CD146^{+}\alpha\text{–}SMA^{+}CD34^{-}PDGFR\beta^{+}NG2^{+}$ pericytes/smooth muscle cells in the microvasculature and adventitial $CD34^{+}CD146^{-}\alpha\text{-}SMA^{-}PDGFR\beta^{-}NG2^{-}$ in larger vessels [31]. In bone marrow, phenotypical differences of perivascular stromal cells/pericytes have been associated with functional differences in hematopoietic stem cells (HSC). Arterioles enclosed by $NG2^{+}$-$Nestin^{bright}$ pericytes have been found associated with quiescent HSCs, while sinusoids harboring $Nestin^{dim}$ $LEPR^{+}$ (leptin receptor) stromal cells/pericytes are in contact with proliferating HSC[32]. In the present study, we did not observe differences in MPC

proliferative activity between different types of vasculature, but we observed proliferation only in CD146$^+$PDGFRβ$^+$ subendothelial MPCs while the adventitia/perivascular CD73$^+$CD271$^+$ PDGFRβ$^+$ population were quiescent. The finding of Ki67$^+$ MPCs in both healthy control and MS tissue was surprising since proliferative activity of cells in the adult brain has so far mainly been shown in endogenous neuronal tissue in both healthy and MS [33, 34]. Our findings are, however, in agreement with Paul et al. who isolated and cultured proliferating perivascular PDGFRβ$^+$Ki67$^+$ cells from healthy brain biopsies, demonstrating tri-lineage differentiation capacity and co-expression of typical MSC (CD90, CD73, CD105, CD29, CD166, and CD49d) and pericyte (PDGFRβ, regulator of G protein signaling 5, CD146, Nestin, α-SMA, and NG2) markers [14]. Flow cytometric analysis of perivascular cells from brain biopsies of persons with epilepsy has also identified PDGFRβ on the majority of cells, while only sub-fractions were reported to express α-SMA, CD73, CD146, and NG2 [15]. Another recent study on stroke tissue from human brains detected the presence of Nestin$^+$α-SMA$^+$NG2$^+$ cells adjacent to the endothelial cell layer, which after isolation expressed Ki67 and PDGFRβ in adherent cell cultures [35].

One major finding in the present study was the loss of subendothelial CD146$^+$ and/or PDGFRβ$^+$ localization in chronic active lesions of both EPMS and LPMS, compared to healthy control tissue. This was not associated with reduced blood vessel numbers since numbers remained unchanged in EPMS and increased in LPMS. PDGFRβ is a tyrosine kinase involved in pericyte recruitment during angiogenesis [36]. Studies in mice with genetically disrupted PDGF/PDGRβ signaling have shown that decreased PDGFRβ immunostaining correlated with a loss of BBB integrity [3]. Reduced immunolocalization of PDGFRβ$^+$ cells in capillaries has also been detected in human and mouse acute ischemic brain tissue [37]. Considering that CD146 is a cell adhesion molecule, the pronounced loss in sub-endothelial distribution of CD146 and PDGFRβ may indicate detachment of pericytes from endothelial cells, although this remains to be determined. Consequently, since the definition of a pericyte includes endothelial cell attachment, the present findings could imply reduced numbers of pericytes [6].

Our results on proliferative activity associated with CD146$^+$PDGFRβ$^+$ cells demonstrate ongoing cell turnover in both MS and healthy brain tissue. It may be hypothesized that in MS, CD146$^+$PDGFRβ$^+$ MPCs change morphology and/or spatial distribution during proliferation as a consequence of the ongoing pathological mechanisms and/or the changed milieu, (Fig. 6). Göritz et al. recently described PDGFRβ$^+$α-SMA$^-$ perivascular cells in mice spinal cord vasculature, which upon injury detached from the vascular wall and gave rise to stromal cells that migrated to the injured site where they participated in regeneration and scarring processes [9]. The migrating scar forming cells ("type A pericytes") were separated from the more abundant desmin$^+$ pericytes in capillaries ("type B pericytes"). These observations are in agreement with our results demonstrating enlarged areas of CD73$^+$CD271$^+$ cells in the adventitia and perivascular cell layers in LPMS. We hypothesize that the increase in adventitial/perivascular CD73$^+$CD271$^+$ immunostaining represent accumulation of differentiated CD73$^+$CD271$^+$stromal cells (similar to type A pericytes) possibly originating from sub-endothelial CD146$^+$PDGFRβ$^+$ MPCs migrating in response to tissue injury.

Independent to the underlying cause, the decrease in CD146$^+$PDGFRβ$^+$ MPCs may contribute to impairments in the BBB. Subtle leakage across the BBB has been found in chronic non-active lesions, which may have a role in progressive MS [38–40]. Interestingly, it was recently shown that inhibition of PDGFR-α signaling using imatinib mesylate (Gleevec) enhanced BBB integrity, reduced CNS inflammation, and ameliorated experimental autoimmune encephalitis disease, suggesting a potential clinical application in MS [41]. Furthermore, brain tissue from mice stroke models displayed loss of PDGFRβ$^+$ pericytes together with the appearance of a new perivascular PDGFRβ$^+$CD105$^+$ cell population [37]. CD105 is a classical marker for culture-expanded bone marrow-derived MSCs, but was not included in the current study since it is abundantly expressed by activated endothelial cells in MS tissue and could obstruct localization of vessel-associated MSCs [21, 42].

Interestingly, LPMS presented with larger CD73$^+$CD271$^+$ adventitial and perivascular regions and increased numbers of blood vessels in active, chronic active, and NAWM compared to healthy brain tissue. CD73 is an extracellular enzyme involved in anti-inflammatory immune responses and has been described to take part in regulation of the BBB [43, 44]. A previous study detected strong CD73 immunoexpression in CD31$^+$ microvasculature in post-mortem MS brain sections [45]. In the present study, CD73 was detected only occasionally in the endothelial cell layer. CD271 (low affinity nerve growth factor receptor) is a receptor for neurotrophins and recognized as a key player in regulation of neuronal cell death and survival but is also involved in immune cell function and chronic neuroinflammation [46–48]. Notably, in line with our study, perivascular CD271$^+$ stromal cells have been found to expand in synovial tissues of rheumatoid arthritis patients [49].

The present detection of enlarged adventitial and perivascular CD73 and CD271 positive areas with colocalization of unchanged PDGFRβ immunoreactivity in LPMS are interesting in view of recent reports suggesting that perivascular PDGFRβ expressing cells are involved in organ fibrosis [50]. Traditionally, resident astroglia were regarded as key effector cells in tissue injury of the CNS but recent studies indicate that stromal cells, originating from perivascular fibroblasts and pericytes, are additional contributors of the fibrotic scar in CNS injury [9, 37, 51]. Our findings of enhanced adventitia and perivascular stromal CD73 and CD271 immunoreactivity in LPMS may be associated with pathologic fibrotic structures that previously have been demonstrated to accumulate in MS lesions, although this remains to be confirmed [52].

Although cultured MSCs have been shown to exhibit remarkable immunosuppressive capabilities, some studies have also pointed out that the immunoregulatory properties of MSCs may depend on culture conditions and on local microenvironment changes [53–55]. If brain MPCs behave in a similar manner to MSCs, it may be suggested that MPCs in the brain of MS patients alter their phenotype and/or function in association with inflammatory activity. The current study of positive immunostaining of HLA-DR that colocalized with C73$^+$CD271$^+$ in active lesions but not in chronic lesions support this hypothesis. In addition, the enlarged C73$^+$CD271$^+$ perivascular areas in LPMS further indicate that MPCs undergo phenotypic changes during the disease course. Additional functional and molecular studies, however, are warranted to investigate this theory and to unravel the physiological relevance of MPCs in healthy and during disease.

The existence of neovascularization in MS has been established but timing of angiogenesis and its pathogenic role remains unclear [56]. In the current study, blood vessel numbers

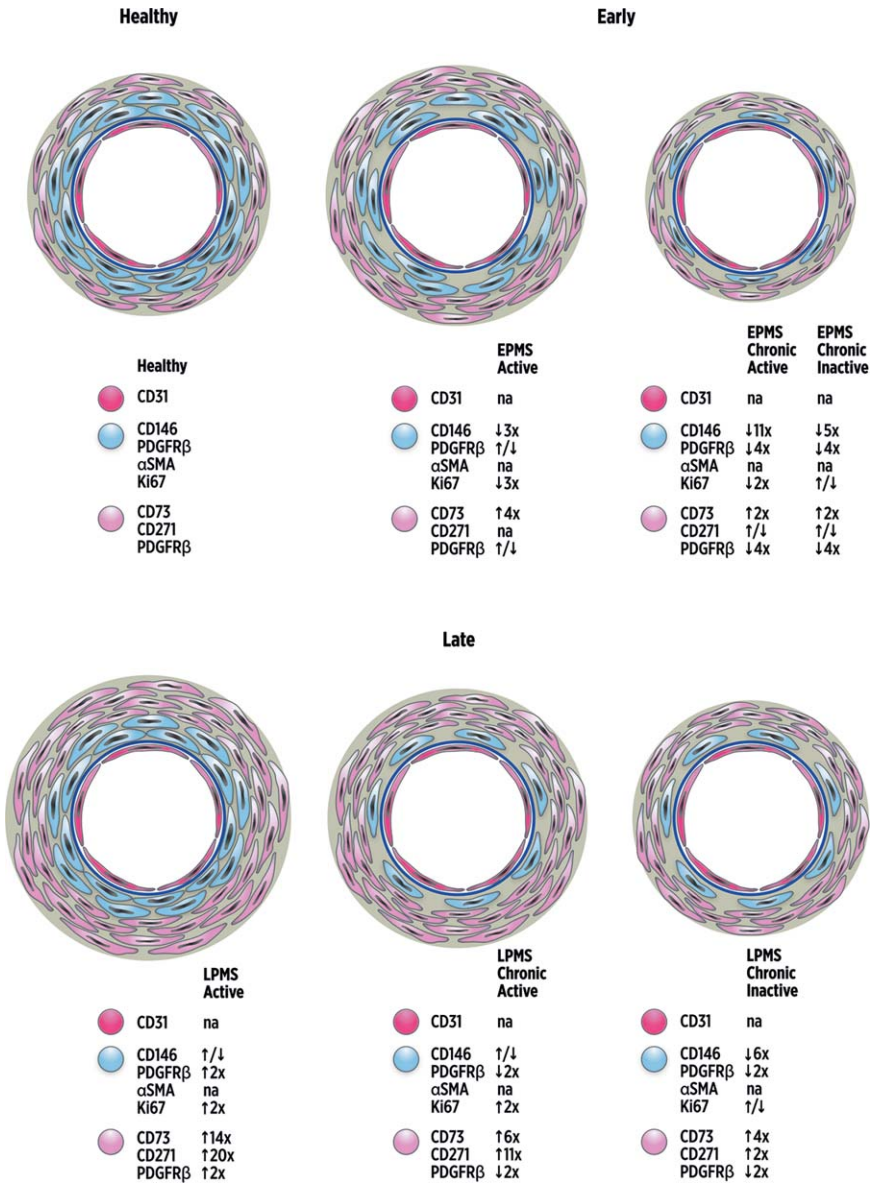

Figure 6. Schematic illustration of the dynamic changes in mesenchymal stromal cells (MSC)/pericyte marker localization with lesion type and multiple sclerosis (MS) disease duration. Schematic representation of vascular and perivascular dynamic changes observed following immunolocalization of MSC/pericyte markers and cell proliferation by Ki67 in MS lesion brain tissues compared to healthy controls. The images also reflect the relative changes in the quantification of immunolocalization compared to healthy tissue, demonstrated by arrows and numbers for each marker (i.e., ↑5x = fivefold increase). $CD146^+PDGFR\beta^+\alpha\text{-}SMA^+Ki67^+$ staining displayed a subendothelial localization (blue cells), separated from the $CD31^+$ endothelial cell layer (dark pink cells) and basement membrane (dark blue circle), with $CD73^+CD271^+PDGFR\beta^+Ki67^-$ staining in the adventitial and perivascular area (light pink cells). Active lesions in early progressive MS (EPMS) tissues presented with decreased immunolocalization of CD146 and Ki67, a similar distribution of PDGFRβ and increased CD73 immunostaining compared to healthy control tissue. CD271 immunostaining was not quantified in EPMS active lesions. EPMS chronic active and chronic inactive lesions both exhibited loss of CD146, and loss of PDGFRβ in chronic active lesions was also seen compared to healthy tissue. CD73 and CD271 were increased in early chronic active but similar in early inactive lesions compared to healthy. However, late stage progressive MS (LPMS) active lesions presented with enlarged regions of PDGFRβ, CD73, CD271, and Ki67 compared to healthy control tissues. LPMS chronic active and chronic inactive lesions showed loss of CD146 and PDGFRβ, but CD73 and CD271 significantly increased in the adventitia and perivascular areas compared to healthy tissue. Ki67 was significantly amplified in chronic active lesions but unchanged in chronic inactive lesions of LPMS compared to healthy tissue. CD31 and α-SMA immunostainings were not quantified (na = not applicable). Abbreviations: α-SMA, alpha-smooth muscle actin; PDGFRβ, platelet-derived growth factor receptor beta.

significantly increased in active, chronic active lesions, and NAWM of LPMS in contrast to LPMS chronic inactive lesions and EPMS, which displayed comparable numbers to healthy tissue.

The age of the healthy group matched EPMS tissue but not LPMS, which may be considered as a limitation in the present study. Age-related pathologies may have contributed to the strong vascular changes in LPMS compared to EPMS and healthy [57]. However, the individual profiles of each pericyte/MSC marker in addition to variations between lesions with different pathologies suggest that factors other than age are involved in the vascular pathologies presented herein. Since our intention was to examine disease progression changes, the differences in average age of

patients in the two MS groups were difficult to avoid. Age-related changes in the brains of older progressive MS patients have previously been recognized as potential contributors to the progression of disease [58].

The mismatch in cause of death between MS cases and healthy donors is a limitation of the study. However, as our study focused on cerebral blood vessels, control subjects and MS patients with a cause of death related to cardiovascular disease were excluded. The detailed neuropathological examination of the healthy control brains had demonstrated that signs of inflammation or vascular abnormalities were absent and helped to avoid other pathologies as confounding factors. The descriptive nature of the current study does not allow for mechanistic conclusions. The relatively small cohort of MS patients and controls is a limitation of the study. We did not separate PPMS from SPMS (in the statistical analyses) since long standing PPMS and SPMS display many clinical and pathological similarities [59]. Larger cohorts of patients are needed to better distinguish differences in MPCs between MS subjects with different disease types and disease duration. However, the multiple tissue regions examined in a considerable number of brain sections and the high number of FoV counted in each region, all contribute to give a good representation of each tissue type investigated.

Conclusion

The current observations of profound cerebral vessel changes including phenotypic alterations of MPCs in progressive MS, in addition to the known functional roles for CD146, PDGFRβ, CD73, and CD271 in neuroinflammation, suggest that MPCs play a role in MS pathology and disease progression. Further studies are warranted to explore the molecular mechanisms involved in the origin of new MPCs and their functions during disease in order to identify new vessel-targeted treatments in progressive MS.

Acknowledgments

We acknowledge the skilled assistance of neuropathology technical staff at University of Turku. Victor Tollemar Wilmenius and Nikolce Tudzarovski (Department of Dental Medicine, Karolinska Institute) for assistance in vessel counting. This work was supported by Stockholm County Council, Swedish Research Council, Max and Edith Follins Foundation, and Karolinska Institutet. E.I. is currently affiliated with the Division of Clinical Immunology, Department of Laboratory Medicine and Department of Clinical Neuroscience, Karolinska Institutet, Stockholm, Sweden.

Author Contributions

E.I.: study conception and design, financial support, data assembly, analysis and interpretation, manuscript writing, final approval of manuscript; R.S.: study conception and design, data assembly, analysis and interpretation, manuscript writing, final approval of manuscript; A.A.T.: study design, data assembly, analysis and interpretation, final approval of manuscript; J.J.A: study conception and design, manuscript writing, final approval of manuscript; H.Q: study conception and design, final approval of manuscript; J.F.: data collection, final approval of manuscript; J.N: provision of study material, data collection, manuscript writing, final approval of manuscript; K.A.: provision of study material, data collection, manuscript writing, final approval of manuscript; H.D.: provision of study material, data collection and manuscript writing, final approval of manuscript; M.R.: study conception and design, provision of study material, data analysis and interpretation, financial support, final approval of manuscript; K.L.B.: study conception and design, financial support, data analysis and interpretation, manuscript writing, final approval of manuscript.

Disclosure of Potential Conflicts of Interest

Katarina Le Blanc is on the Board of Directors of Cell Protect and is co-founder and owner of iCell Science. The other authors indicated no potential conflicts of interest.

References

1 Compston A, Coles A. Multiple sclerosis. Lancet 2002;359:1221–1231.

2 Ballabh P, Braun A, Nedergaard M. The blood-brain barrier: An overview: Structure, regulation, and clinical implications. Neurobiol Dis 2004;16:1–13.

3 Armulik A, Genove G, Mae M et al. Pericytes regulate the blood-brain barrier. Nature 2010;468:557–561.

4 Engelhardt B. The blood-central nervous system barriers actively control immune cell entry into the central nervous system. Curr Pharm Des 2008;14:1555–1565.

5 Frank RN, Dutta S, Mancini MA. Pericyte coverage is greater in the retinal than in the cerebral capillaries of the rat. Invest Ophthalmol Vis Sci 1987;28:1086–1091.

6 Shepro D, Morel NM. Pericyte physiology. FASEB J 1993;7:1031–1038.

7 Bell RD, Winkler EA, Sagare AP et al. Pericytes control key neurovascular functions and neuronal phenotype in the adult brain and during brain aging. Neuron 2010;68:409–427.

8 Persidsky Y, Hill J, Zhang M et al. Dysfunction of brain pericytes in chronic neuroinflammation. J Cereb Blood Flow Metab 2015;36:794–807.

9 Goritz C, Dias DO, Tomilin N et al. A pericyte origin of spinal cord scar tissue. Science 2011;333:238–242.

10 Doherty MJ, Ashton BA, Walsh S et al. Vascular pericytes express osteogenic potential in vitro and in vivo. J Bone Miner Res 1998;13:828–838.

11 Farrington-Rock C, Crofts NJ, Doherty MJ et al. Chondrogenic and adipogenic potential of microvascular pericytes. Circulation 2004;110:2226–2232.

12 Dore-Duffy P, Katychev A, Wang X et al. CNS microvascular pericytes exhibit multipotential stem cell activity. J Cereb Blood Flow Metab 2006;26:613–624.

13 Crisan M, Yap S, Casteilla L et al. A perivascular origin for mesenchymal stem cells in multiple human organs. Cell Stem Cell 2008;3:301–313.

14 Paul G, Ozen I, Christophersen NS et al. The adult human brain harbors multipotent perivascular mesenchymal stem cells. PLoS One 2012;7:e35577.

15 Lojewski X, Srimasorn S, Rauh J et al. Perivascular mesenchymal stem cells from the adult human brain harbor no instrinsic neuroectodermal but high mesodermal differentiation potential. Stem Cells Transl Med 2015;4:1223–1233.

16 Nauta AJ, Fibbe WE. Immunomodulatory properties of mesenchymal stromal cells. Blood 2007;110:3499–3506.

17 Connick P, Kolappan M, Crawley C et al. Autologous mesenchymal stem cells for the treatment of secondary progressive multiple sclerosis: An open-label phase 2a proof-of-concept study. Lancet Neurol 2012;11:150–156.

18 Le Blanc K, Frassoni F, Ball L et al. Mesenchymal stem cells for treatment of steroid-resistant, severe, acute graft-versus-host disease: A phase II study. Lancet 2008;371:1579–1586.

19 Zappia E, Casazza S, Pedemonte E et al. Mesenchymal stem cells ameliorate experimental autoimmune encephalomyelitis

inducing T-cell anergy. Blood 2005;106:1755–1761.

20 Zhang J, Li Y, Lu M et al. Bone marrow stromal cells reduce axonal loss in experimental autoimmune encephalomyelitis mice. J Neurosci Res 2006;84:587–595.

21 Dominici M, Le Blanc K, Mueller I et al. Minimal criteria for defining multipotent mesenchymal stromal cells. The International Society for Cellular Therapy position statement. Cytotherapy 2006;8:315–317.

22 Maier CL, Shepherd BR, Yi T et al. Explant outgrowth, propagation and characterization of human pericytes. Microcirculation 2010;17:367–380.

23 Murfee WL, Skalak TC, Peirce SM. Differential arterial/venous expression of NG2 proteoglycan in perivascular cells along microvessels: Identifying a venule-specific phenotype. Microcirculation 2005;12:151–160.

24 Nehls V, Drenckhahn D. Heterogeneity of microvascular pericytes for smooth muscle type alpha-actin. J Cell Biol 1991;113:147–154.

25 Sugars RV, Olsson ML, Marchner S et al. The glycosylation profile of osteoadherin alters during endochondral bone formation. Bone 2013;53:459–467.

26 Carpenter AE, Jones TR, Lamprecht MR et al. CellProfiler: Image analysis software for identifying and quantifying cell phenotypes. Genome Biol 2006;7:R100.

27 Zeger SL, Liang KY, Albert PS. Models for longitudinal data: A generalized estimating equation approach. Biometrics 1988;44:1049–1060.

28 Kamouchi M, Ago T, Kitazono T. Brain pericytes: Emerging concepts and functional roles in brain homeostasis. Cell Mol Neurobiol 2011;31:175–193.

29 Lassmann H, Raine CS, Antel J et al. Immunopathology of multiple sclerosis: Report on an international meeting held at the Institute of Neurology of the University of Vienna. J Neuroimmunol 1998;86:213–217.

30 da Silva Meirelles L, Caplan AI, Nardi NB. In search of the in vivo identity of mesenchymal stem cells. Stem Cells 2008;26:2287–2299.

31 Corselli M, Chen CW, Sun B et al. The tunica adventitia of human arteries and veins as a source of mesenchymal stem cells. Stem Cells Dev 2012;21:1299–1308.

32 Kunisaki Y, Frenette PS. Influences of vascular niches on hematopoietic stem cell fate. Int J Hematol 2014;99:699–705.

33 Johansson CB, Svensson M, Wallstedt L et al. Neural stem cells in the adult human brain. Exp Cell Res 1999;253:733–736.

34 Snethen H, Love S, Scolding N. Disease-responsive neural precursor cells are present in multiple sclerosis lesions. Regen Med 2008;3:835–847.

35 Tatebayashi K, Tanaka Y, Nakano-Doi A et al. Identification of multipotent stem cells in human brain tissue following stroke. Stem Cells Dev 2017;26:787–797.

36 Zhang J, Cao R, Zhang Y et al. Differential roles of PDGFR-alpha and PDGFR-beta in angiogenesis and vessel stability. FASEB J 2009;23:153–163.

37 Fernandez-Klett F, Potas JR, Hilpert D et al. Early loss of pericytes and perivascular stromal cell-induced scar formation after stroke. J Cereb Blood Flow Meta 2013;33:428–439.

38 Claudio L, Raine CS, Brosnan CF. Evidence of persistent blood-brain barrier abnormalities in chronic-progressive multiple sclerosis. Acta Neuropathol 1995;90:228–238.

39 Leech S, Kirk J, Plumb J et al. Persistent endothelial abnormalities and blood-brain barrier leak in primary and secondary progressive multiple sclerosis. Neuropathol Appl Neurobiol 2007;33:86–98.

40 Nishihara H, Shimizu F, Kitagawa T et al. Identification of galectin-3 as a possible antibody target for secondary progressive multiple sclerosis. Mult Scler 2017;23:382–394.

41 Adzemovic MV, Zeitelhofer M, Eriksson U et al. Imatinib ameliorates neuroinflammation in a rat model of multiple sclerosis by enhancing blood-brain barrier integrity and by modulating the peripheral immune response. PLoS One 2013;8:e56586.

42 Holley JE, Newcombe J, Whatmore JL et al. Increased blood vessel density and endothelial cell proliferation in multiple sclerosis cerebral white matter. Neurosci Lett 2010;470:65–70.

43 Mills JH, Thompson LF, Mueller C et al. CD73 is required for efficient entry of lymphocytes into the central nervous system during experimental autoimmune encephalomyelitis. Proc Natl Acad Sci USA 2008;105:9325–9330.

44 Bynoe MS, Viret C, Yan A et al. Adenosine receptor signaling: A key to opening the blood-brain door. Fluids Barriers CNS 2015;12:20.

45 Niemela J, Ifergan I, Yegutkin GG et al. IFN-beta regulates CD73 and adenosine expression at the blood-brain barrier. Eur J Immunol 2008;38:2718–2726.

46 Barker PA. p75NTR is positively promiscuous: Novel partners and new insights. Neuron 2004;42:529–533.

47 Dowling P, Ming X, Raval S et al. Up-regulated p75NTR neurotrophin receptor on glial cells in MS plaques. Neurology 1999;53:1676–1682.

48 Valdo P, Stegagno C, Mazzucco S et al. Enhanced expression of NGF receptors in multiple sclerosis lesions. J Neuropathol Exp Neurol 2002;61:91–98.

49 Del Rey MJ, Fare R, Usategui A et al. CD271(+) stromal cells expand in arthritic synovium and exhibit a proinflammatory phenotype. Arthritis Res Ther 2015;18:66.

50 Humphreys BD, Lin SL, Kobayashi A et al. Fate tracing reveals the pericyte and not epithelial origin of myofibroblasts in kidney fibrosis. Am J Pathol 2010;176:85–97.

51 Faulkner JR, Herrmann JE, Woo MJ et al. Reactive astrocytes protect tissue and preserve function after spinal cord injury. J Neurosci 2004;24:2143–2155.

52 Mohan H, Krumbholz M, Sharma R et al. Extracellular matrix in multiple sclerosis lesions: Fibrillar collagens, biglycan and decorin are upregulated and associated with infiltrating immune cells. Brain Pathol 2010;20:966–975.

53 Schafer R, Spohn G, Baer PC. Mesenchymal stem/stromal cells in regenerative medicine: Can preconditioning strategies improve therapeutic efficacy? Transfus Med Hemother 2016;43:256–267.

54 Del Rey MJ, Fare R, Usategui A et al. CD271(+) stromal cells expand in arthritic synovium and exhibit a proinflammatory phenotype. Arthritis Res Ther 2016;18:66.

55 Kizilay Mancini O, Lora M, Shum-Tim D et al. A proinflammatory secretome mediates the impaired immunopotency of human mesenchymal stromal cells in elderly patients with atherosclerosis. Stem Cells Transl Med 2017;6:1132–1140.

56 Lengfeld J, Cutforth T, Agalliu D. The role of angiogenesis in the pathology of multiple sclerosis. Vascular Cell 2014;6:23.

57 Bianchi E, Ripandelli G, Taurone S et al. Age and diabetes related changes of the retinal capillaries: An ultrastructural and immunohistochemical study. Int J Immunopathol Pharmacol 2016;29:40–53.

58 Mahad DH, Trapp BD, Lassmann H. Pathological mechanisms in progressive multiple sclerosis. Lancet Neurol 2015;14:183–193.

59 Antel J, Antel S, Caramanos Z et al. Primary progressive multiple sclerosis: Part of the MS disease spectrum or separate disease entity? Acta Neuropathol 2012;123:627–638.

See www.StemCellsTM.com for supporting information available online.